ELSEVIER

Biophysical Chemistry 62 (1996) 63–72

Biophysical Chemistry

Chemisorption of proteins and their thiol derivatives onto gold surfaces: characterization based on electrochemical nonlinearity

Satoshi Nakata [a,*], Naoko Kido [a], Mami Hayashi [a], Masahiko Hara [b], Hiroyuki Sasabe [b], Takashi Sugawara [c], Takehisa Matsuda [c]

[a] *Department of Chemistry, Nara University of Education, Takabatake-cho, Nara 630, Japan*
[b] *Frontier Research Program, The Institute of Physical and Chemical Research, Wako, Saitama 351-01, Japan*
[c] *Department of Bioengineering, National Cardiovascular Center Research Institute, Suita, Osaka 565, Japan*

Received 15 February 1996; accepted 22 July 1996

Abstract

This study was conducted to monitor the electrochemical responses of two proteins (bovine serum albumin (BSA) and gelatin) and their thiol derivatives adsorbed onto gold (Au) electrodes, which were analyzed by a "nonlinear" impedance method. A sinusoidal voltage is applied to a protein-containing aqueous solution and the waveform of the output current is analyzed by fast Fourier transformation (FFT). The intensities of the higher harmonics in the FFT varied with the species of protein and their thiol derivatives, and with time. From the higher harmonics, voltage-dependent capacitance and conductance were quantitatively evaluated to differentiate the state of adsorbed protein. Adsorption and desorption characteristics of BSA and its thiol derivative on the Au surface were continuously measured by a quartz crystal microbalance (QCM) in situ. The microscopic state of thiol-derivatized BSA adsorbed onto the Au surface was imaged by atomic force microscopy (AFM). In general, thiol-derivatized proteins were tightly adsorbed on the Au surface and showed no desorption. The present electrochemical measurements clearly differentiated adsorption characteristics of physically adsorbed (physisorbed) and chemically adsorbed (chemisorbed) proteins on Au surfaces.

Keywords: Bovine serum albumin; Gelatin; Nonlinearity; Alkanethiol; Gold surface; Chemisorption

1. Introduction

Chemical composition, structure and properties of the blood- and tissue-contacting surfaces of medical devices play a decisive role in their protein adsorption behavior which, in turn, determines the biocompatibility of the devices [1,2]. Therefore, an understanding of protein adsorption dynamics and the physicochemical state of an adsorbed protein on a solid surface is essential for the development of biological fluid-contacting devices such as artificial hearts, blood vessels and biosensors [1–6]. When a protein is preadsorbed on a device surface, such a physically adsorbed protein may be desorbed and replaced by a different species of protein present in biological fluid in vivo as well as in vitro. On the other hand, covalent bonding of a protein onto a substrate, which is generally achieved by condensation between functional groups of a protein and a

* Corresponding author. Tel: +81-742-27-9191; Fax: +81-742-27-9190; E-mail: nakatas@nara-edu.ac.jp

PII S0301-4622(96)02208-9

substrate, is essentially resistant to desorption, forming a stable proteinaceous layer on the device surface.

Recent studies have shown that the chemisorption of alkanethiols onto metals such as gold, silver, platinum and copper occurs to form a self-assembling membrane (SAM) [7–12]. It is assumed that the bond energy between gold and the sulfur of thiol is much larger than that due to hydrogen bonding and electrostatic interaction. Thus, it is expected that such a chemisorbed protein will be stable under physiological conditions. Therefore, the state of the chemisorbed protein might be different from that of the physically adsorbed protein. Although there have been various methods for determining the molecular process of protein adsorption onto a solid surface, few methods have been available for in situ continuous monitoring. Quantitative techniques based on electrochemical measurements have been introduced recently [5,6,13]. It is difficult to determine the physicochemical state of adsorbed proteins on surfaces.

We have recently reported a novel sensing method for detecting the physicochemical state at a solution–metal interface, the nonlinear impedance method [14]. It is based on the detection of electrochemical information of higher harmonics in the fast Fourier Transformation (FFT) of an output current under the application of an external sinusoidal voltage as shown in Fig. 1. Voltage-dependent conductance and capacitance (differential capacitance), which are evaluated from the real part and the imaginary part of the FFT, respectively, correspond to the conductance of molecules adsorbed on the electrode and the diffuse double layer around the electrode, respectively [14–17]. It has been demonstrated that this method has excellent reproducibility and affords much useful information on the electrochemical system [15]. In fact, the adsorption characteristics of bovine serum albumin onto a platinum electrode were electrochemically determined by this technique, indicating that the intensities of the power spectrum of higher harmonics change with the concentration and with time [14].

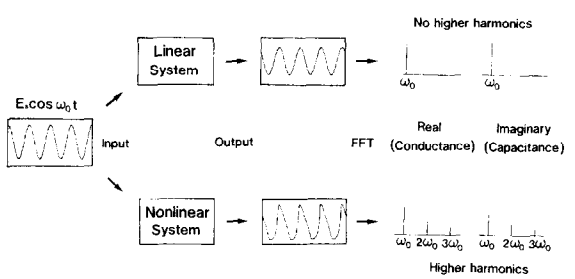

Fig. 1. Schematic representation of the mechanism for evaluating electrochemical nonlinearity. Higher harmonics of the real part and those of the imaginary part in FFT correspond to the nonlinear conductance and the nonlinear capacitance in the electrochemical system, respectively.

In this paper, adsorption characteristics of proteins with or without the thiol group on an Au electrode were monitored by nonlinear impedance measurement. Voltage-dependent changes in the intensities of the higher harmonics in FFT as functions of protein concentration and time clearly differentiated between the chemisorbed and physisorbed proteins. The adsorption characteristics and state of protein adsorbed on the Au surface were also measured using a quartz crystal microbalance (QCM) and imaged by atomic force microscopy (AFM). These results are discussed in relation to the difference between the adsorption mechanisms.

2. Experimental

2.1. Electrochemical instrument

The test solution consisted of 0.1369 M NaCl, 0.0268 M KCl, 0.00958 M Na_2HPO_4 and 0.00146 M KH_2PO_4 and was buffered at pH 7.4. Water was first distilled and then purified with a Millipore Milli-Q filtering system. Electrical measurements were performed using the apparatus shown in Fig. 2 [14]. Sinusoidal voltage (frequency 0.5 Hz, amplitude 0.3 V) was generated by a potentiostat (HA-10 RIG, Hokuto Denko Ltd., Japan) connected to a waveform generator (Model 459 AL, Kikusui Electronics Corp., Japan). The input sinusoidal potential and the output current were stored in a personal computer (NEC 9801, NEC Co. Ltd., Japan), and then Fourier-transformed to the frequency domain. A gold wire (length 10 mm, diameter 0.5 mm), a Ag/AgCl electrode and a platinum wire (length 40

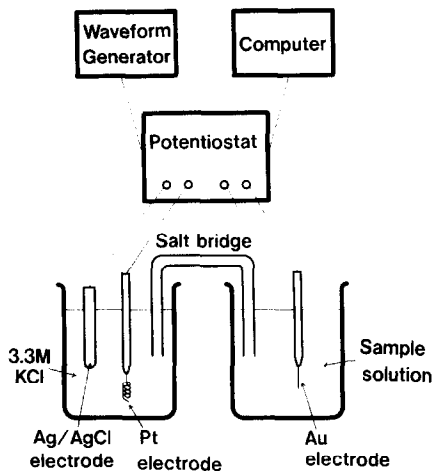

Fig. 2. Diagram of the experimental apparatus for measuring electrochemical nonlinearity.

mm, diameter 0.5 mm) were used as the working electrode, the reference electrode and the current electrode, respectively. All measurements were performed at 298 ± 1 K.

2.2. Atomic force microscopy (AFM)

The AFM system used in this study was a commercial microscope, Nanoscope II (Digital Instruments, Santa Barbara, USA). An Si_3N_4 cantilever (length 200 μm, V-type shape) with a force constant of 0.06 N m^{-1} was scanned over the sample in pure air at room temperature. A 50-nm Au film used as the substrate in AFM was obtained by electric melting of a gold rod (purity 99.999%), evaporation on a mica wafer and annealing under vacuum (10^{-7} torr) [18].

2.3. Quartz crystal microbalance (QCM)

Quartz crystals (purchased from Seiko Electric Company Ltd., Tokyo, Japan) consisted of AT-cut quartz (diameter 5 mm) with a basic resonant frequency of 9 MHz [13,19–21], the surface of which was coated with Au by vapor deposition. By sealing the quartz with a silicone cell, only one side of the Au surface was in contact with the test solution (volume 100 ml). Tris buffer solution (0.05 M) was used for the QCM.

2.4. Proteins

Bovine serum albumin (BSA) and gelatin were obtained from Miles Laboratories, Inc. (Chicago, USA) and Wako Chemicals (Kyoto, Japan), respectively. Thiol-derivatized BSA and gelatin (designated as SH–BSA and SH–gelatin) were prepared as follows. A mixed aqueous solution of 3-mercaptopropionic acid (0.50 g, 4.2 mmol), protein (2 g) and a water-soluble carbodiimide (1.0 g, 5 mmol) was kept in an ice–water bath and stirred for 1 day, and then dialyzed against distilled water using a cellulose tube for 4 days. White powdery proteins were obtained after lyophilization. The number of incorporated thiol groups per molecule was determined as approximately 6.2 for BSA and 7.0 for gelatin by titration of the primary amino group of lysine residues of a protein molecule using the trinitrobenzene sulfonic acid method [22].

3. Results

3.1. Electrochemical nonlinear responses upon adsorption

The measurement of electrochemical nonlinearity upon protein adsorption on the Au electrode was carried out in a phosphate-buffered solution (PBS) using the electrochemical measuring apparatus and analyzing instrument as shown in Fig. 2. Proteins used were nonmodified BSA and gelatin, and their thiol derivatives (SH–BSA and SH–gelatin), both of which were prepared by condensation of 3-mercaptopropionic acid with the lysine residue of the corresponding protein. Both proteins contained around 6–7 thiol groups per molecule.

Fig. 3 shows the time variations of the output current versus input sinusoidal voltage (i–v) curves in protein-containing PBS (protein concentration 1 mg ml^{-1}, measurement time 10, 30 and 60 min after immersion of the electrode in the solution). Irrespective of the species of protein, a large amplitude and a large degree of hysteresis in the i–v loop were observed for nonmodified proteins, whereas a much smaller amplitude and a smaller degree of hysteresis in the i–v loop were observed for both thiol-derivatized proteins. Although differences in i–v curves

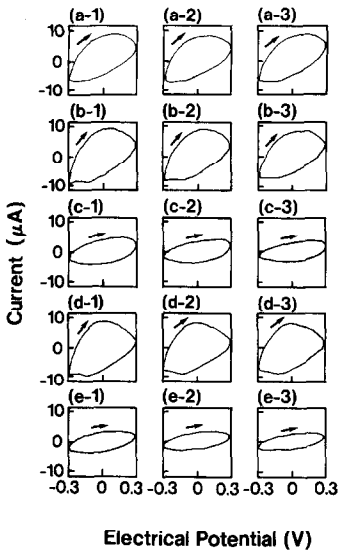

Fig. 3. Current (i) versus electrical potential (V) curves for (a) PBS without proteins, (b) gelatin, (c) SH–gelatin, (d) BSA and (e) SH–BSA after the elapsed time of (1) 10 min, (2) 30 min and (3) 60 min. The concentration of each protein was 1 mg ml^{-1} in PBS.

between the nonmodified proteins and between the thiol-derivatized proteins and their time-variation changes appeared to be small, electrochemical nonlinearity analyzed using higher harmonics of FFT clearly differentiated between the electrochemical responses of these proteins as will be shown below.

If the system has a linear property, the i–v curve is ellipsoidal and there are no higher harmonics in FFT as shown in Fig. 1. The appearances of the deformation of current versus voltage curve and the higher harmonics are due to the electrochemical nonlinearity [14–17,23]. Relative intensities of higher harmonics to the fundamental harmonic of the power spectrum, R_2/P_1 and I_2/P_1, were adopted as indices of nonlinearity: R_2 and I_2 are the intensities of the second harmonic in the real and imaginary parts, respectively, P_1 is the intensity of the power spectrum ($=(R_1^2+I_1^2)^{1/2}$) and 0.5 Hz is the frequency of the fundamental harmonic. Reproducibility of the conventional impedance method is poor because measured values varied largely even with a slight dimensional change in the distance between electrodes, the presence of impurities such as bubbles on the electrode and the aging arising from the adsorption of various electrolytes on the electrode at the lower frequency [24,25]. In addition, our study showed that the linear components have relatively large experimental errors (approximately 20%) in each experimental run, whereas the normalization to P_1 reduced errors to within 5% for all measurements in this study.

Fig. 4 shows the time dependence of the relative intensity of higher harmonics in FFT of the output current. The analyzed data correspond to the current values in Fig. 3 (protein concentration 1 mg ml^{-1}). Even in the absence of protein in PBS, the higher harmonics appeared significantly. However, little time-dependent change in R_2/P_1 was observed for the protein-free PBS, whereas significant time-dependent change was observed for protein solutions. These results indicated that, irrespective of the species of protein, both thiol-derivatized proteins provided much larger intensities of R_2/P_1 and I_2/P_1 than the corresponding nonmodified proteins. Regardless of the species of protein and thiol modification, an increase in intensity was observed at an early period of immersion, whereas it eventually remained constant after longer periods of immersion. Upon thorough washing with distilled water, little change in R_2/P_1 and I_2/P_1 was observed for both thiol-derivatized proteins, whereas a significant change of these parameters was observed for nonmodified ones.

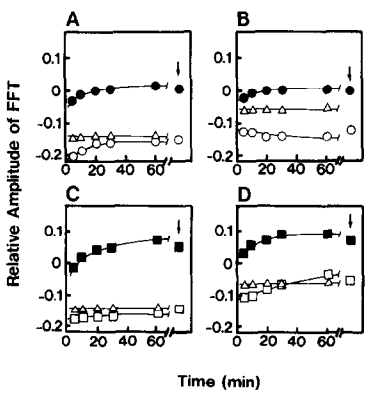

Fig. 4. Time-dependent change of relative intensity of higher harmonics (A and C, R_2/P_1; B and D, I_2/P_1) for BSA (○), SH–BSA (●), gelatin (□), SH–gelatin (■) and PBS without protein (△). The analyzed data correspond to the current values in Fig. 3. The point marked by an arrow in each figure indicates the value obtained after five times immersion of the protein-adsorbed Au electrode in PBS.

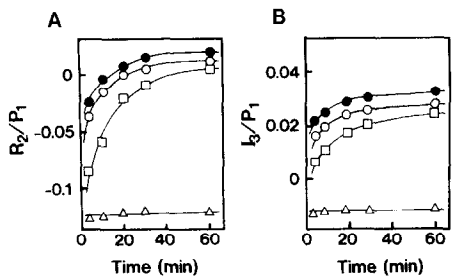

Fig. 5. Time-dependent change of relative intensity of higher harmonics (A) R_2/P_1 and (B) I_3/P_1 at various concentrations of SH–BSA: (△) PBS only; (□) 0.1 mg ml^{-1}; (○) 0.5 mg ml^{-1}; (●) 1 mg ml^{-1}.

Fig. 5 shows the time variation of the relative intensities of higher harmonics, R_2/P_1 and I_3/P_1, at different concentrations of SH–BSA. Little time-dependent change in R_2/P_1 and I_3/P_1 was observed for the protein-free PBS, whereas time-dependent increases in both indices were observed for protein-containing solutions: the higher the concentration was varied, the much larger change was observed at an earlier period of immersion. I_3/P_1 was plotted in Fig. 5 since this relative intensity significantly depended on the concentration of SH–BSA (note that I_2/P_1 of SH–BSA is almost zero in Fig. 4). The physicochmical meaning of higher harmonics is discussed in the following theoretical section. Thus, voltage-dependent conductance and capacitance afford information on not only the qualitative adsorption state but also the quantitative adsorption rate.

3.2. Theoretical analysis of electrochemical nonlinear responses

In order to evaluate the electrochemical nonlinear responses, the differential capacitance and conductance were estimated from higher harmonics as electrochemical elements [14–17,23,26]. Let us assume differential capacitance (C) and conductance (G) as simple nonlinear elements given by Eqs. (1) and (2):

$$C(V) = C_0 + C_1V + C_2V^2 + C_3V^3 \quad (1)$$

$$G(V) = G_0 + G_1V + G_2V^2 + G_3V^3 \quad (2)$$

When a sinusoidal potential ($V(t) = E_a \cos \omega_0 t$, where $E_a = 0.3$ V, $\omega_0 = 2\pi f$, $f = 0.5$ Hz) is applied to a parallel circuit with nonlinear capacitance and nonlinear conductance, as expressed in Eqs. (1) and (2), the output current, $I(t)$, at a given time is given by Eq. (3) (for a detailed derivation, see Appendix A and our previous papers [14,15]).

$$\begin{aligned} I(t) = {} & 4.5 \times 10^{-2} G_1 + 3.0375 \times 10^{-3} G_3 \\ & + (0.3G_0 + 2.025 \times 10^{-2} G_2)\cos \omega_0 t \\ & + (4.5 \times 10^{-2} G_1 \\ & + 4.05 \times 10^{-3} G_3)\cos 2\omega_0 t \\ & + 6.75 \times 10^{-3} G_2 \cos 3\omega_0 t \\ & + 1.0125 \times 10^{-3} G_3 \cos 4\omega_0 t \\ & - 0.3\pi\{(C_0 + 2.25 \times 10^{-2} C_2)\sin \omega_0 t \\ & + (0.15C_1 + 6.75 \times 10^{-3} C_3)\sin 2\omega_0 t \\ & + 2.25 \times 10^{-2} C_2 \sin 3\omega_0 t \\ & + 3.375 \times 10^{-3} C_3 \sin 4\omega_0 t\} \end{aligned} \quad (3)$$

When the current $I(t)$ is Fourier-transformed, the coefficients of the cosine and sine functions correspond to the real and imaginary parts, respectively. From Eq. (3), it is apparent that the second, third and fourth harmonics of the real and imaginary parts are related to the first, second and third derivatives in the nonlinear conductance and nonlinear capacitance, as follows:

$$R_1 = 0.3G_0 + 2.025 \times 10^{-2} G_2$$

$$R_2 = 4.5 \times 10^{-2} G_1 + 4.05 \times 10^{-3} G_3$$

$$R_3 = 6.75 \times 10^{-3} G_2$$

$$R_4 = 1.0125 \times 10^{-3} G_3$$

$$I_1 = \pi(0.3C_0 + 6.75 \times 10^{-3} C_2)$$

$$I_2 = \pi(4.5 \times 10^{-2} C_1 + 2.025 \times 10^{-3} C_3)$$

$$I_3 = 6.75 \times 10^{-3} \pi C_2$$

$$I_4 = 1.0125 \times 10^{-3} \pi C_3$$

Fig. 6 shows differential capacitance and voltage-dependent conductance which were computer-simulated using the experimental data of the Fourier transformation of the output current shown in Fig. 3(3) (the elapsed time of measurement was 60

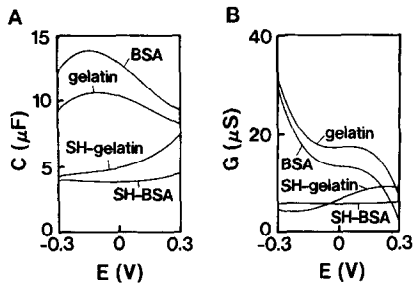

Fig. 6. (A) Differential capacitance and (B) voltage-dependent conductance evaluated from the Fourier transformation of the output currents and the model of the parallel circuit of resistor and condenser. The simulated output currents are (b-3), (c-3), (d-3) and (e-3) in Fig. 3 (measurement time, 60 min; protein concentration, 1 mg ml^{-1} in PBS).

min, protein concentration 1 mg ml^{-1}), where the components of the second, third and fourth harmonics were evaluated using Eq. (3). Note that the nonlinearity of capacitance and conductance depends on the species and thiol modification. In particular, thiol modification, irrespective of the species of protein, not only lowered the capacitance and conductance markedly, but also changed their voltage dependency considerably. For example, the slopes of capacitance–electrical potential curves for thiol-derivatized proteins are positive at positive potential, but the slopes for nonmodified proteins are negative, as seen in Fig. 6. In addition, C_1 values in SH–gelatin and SH–BSA are positive and almost zero, respectively. C_1 is related to I_2/P_1, as deduced in Eq. (3). Indeed, I_2/P_1 values in SH–gelatin and SH–BSA are positive and almost zero, respectively, in Fig. 4. According to the Gouy–Chapman theory, both C_1 and C_3 are zero in an electrolyte with a symmetrical charge magnitude, e.g. NaCl or $CaSO_4$ [26]. On the other hand, C_1 and C_3 have some value in an asymmetrical electrolyte. The difference in C_1 between SH–gelatin and SH–BSA may be due to the location of positively and negatively charged domains in the proteins.

In the non-fixed form proteins (BSA and gelatin), the electrochemical nonlinearity on the bulk phase is generated by the presence of diffuse double layers of inorganic ions in addition to the adsorption of proteins on the electrode surface, and then the differential capacitance of BSA seems to be similar to that of gelatin. In contrast, the resistance of the electrode surface is increased by the strong adsorption of thiol-derivatized proteins, and then the information on the electrode surface is selectively detected in the fixed form proteins.

In the present experiment, we used a sinusoidal potential with a single frequency (0.5 Hz). Our model is preliminary since the present simulation is based on the assumption that the capacitance is independent of potential sweep rate. As hysteresis on the i–v curve is generated in the formation of a double layer, the differential capacitance may depend on the scan rate of the potential or the applied frequency. The effect of the potential sweep rate should be included as a development of this simulation.

3.3. QCM measurement during protein adsorption and desorption

The QCM, which is very sensitive to mass change on a solid surface [13,19–21], was used for measuring the mass of SH–BSA and BSA adsorbed on the gold surface. A thin-film Au-deposited quartz crystal electrode was immersed in a Tris-buffered solution containing SH–BSA or BSA for up to 80 min, and then transferred to a protein-free PBS. During the experiment, the frequency of the oscillating crystal was continuously monitored (Fig. 7). In this experiment, the frequency jump was observed at the arrow points in Fig. 7. The plot of the frequency jump was omitted since the frequency was almost restored within several tens of seconds after the exchange of the sample solution. A decrease in the frequency indicates an increase in the mass on the electrode

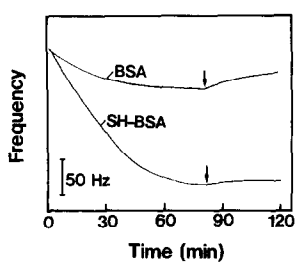

Fig. 7. Typical time-dependent change in the frequency of SH–BSA and BSA adsorption and desorption on Au-coated quartz crystal oscillators. SH–BSA (1 mg ml^{-1}) or BSA (1 mg ml^{-1}) in 0.05 M Tris-buffered solution was used. The probe was transferred to PBS without BSA or SH–BSA at the time indicated by the downward arrow.

(note that a decrease of 1 Hz corresponds to an increase of 1 ng). Compared with BSA, a rapid increase in mass occurred with SH–BSA at an early period of incubation. For both proteins, the decrease in frequency was stabilized within 1 h incubation, reaching an equilibrium state. The difference in frequency at an equilibrium state showed that the amount of adsorbed protein was larger for SH–BSA than for BSA. On transferring the probe to a protein-free PBS for SH–BSA, the oscillatory frequency remained almost unchanged, whereas the frequency increased for BSA. These results indicate that little desorption occurred for SH–BSA adsorbed on an Au surface whereas BSA adsorbed on an Au surface desorbed with time.

3.4. Atomic force micrograph of SH–BSA adsorbed on an Au surface

AFM was used for observing SH–BSA adsorbed on a regionally well-crystallized gold surface, which was prepared by a high-vacuum deposition technique [12,18,27]. Fig. 8 shows the AFM images for gold surfaces subjected to immersion in different concentrations (1×10^{-2}–1 mg ml^{-1}) of SH–BSA for 1 h and subsequent thorough washing with distilled water. At the lowest concentration (1×10^{-2} mg ml^{-1}), the proteins tended to adsorb regionally, resulting in the formation of relatively deformed and large aggregates which were randomly scattered on the surface at a low density. At an intermediate concentration

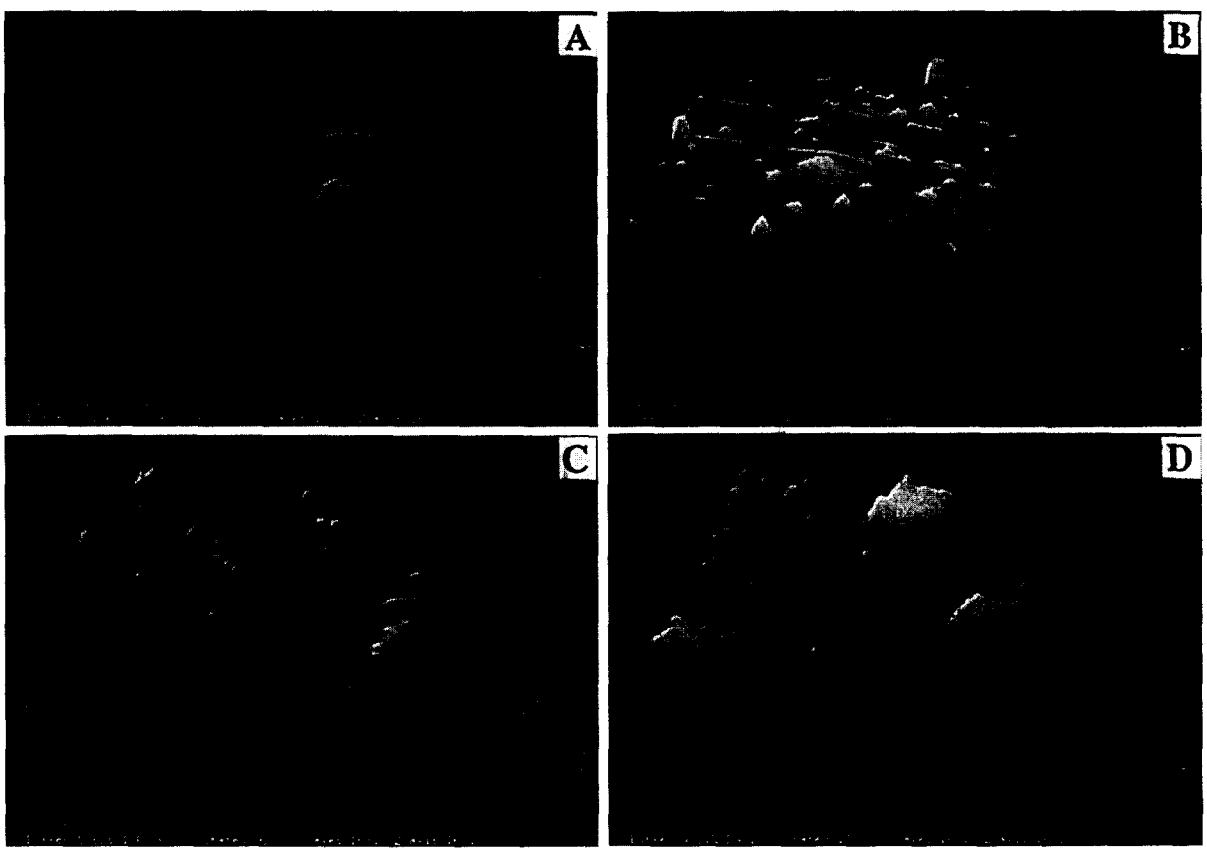

Fig. 8. AFM images for SH–BSA adsorbed on an Au surface. The probes, which were immersed in (A) purified water without protein, (B) 0.01, (C) 0.1 and (D) 1 mg ml^{-1} SH–BSA aqueous solution for 1 h, were washed in purified water five times, then measured in air.

(0.1 mg ml^{-1}), small spherical aggregates of proteins completely covered the gold surfaces. At the highest concentration (0.1 mg ml^{-1}) a thick, continuous proteinaceous layer was formed, which appeared to be composed of spherical aggregates.

4. Discussion

Information on the dynamic adsorption process and the adsorption state of proteins on material surfaces may provide a solid basis for the logical surface design of devices which come into contact with biological fluids such as blood. A variety of spectroscopic techniques has been developed to monitor the kinetics of adsorption of proteins onto materials [1]. These include IR spectroscopy, fluorescence spectroscopy, total internal reflection fluorescence and ellipsometry. However, most of these techniques measure the amount of adsorbed protein. Circular dichroism can provide information on relatively large conformational changes upon adsorption. On the other hand, electrochemical techniques, which have been developed recently, allow reproducible, continuous in situ measurements of protein adsorption with much higher sensitivity than spectroscopic techniques.

The electrochemical techniques consist of an impedance method which was introduced by Caprani and co-workers [13] in 1993 and by us [15] in 1989, and a QCM method which enables determination of the amount of adsorbed proteins with very high time-resolution [19,20]. Caprani and co-workers proposed the measurement of double-layer capacitance which can be directly calculated from the imaginary part of the impedance measured at a single frequency [13]. The method allows reproducible in situ measurements with a time resolution of 0.1 s. Using this technique, kinetic characteristics of protein adsorption on a gold electrode were recorded precisely for up to several minutes after immersion in protein-containing solutions, and a model of the time-dependent interfacial structure of a proteinaceous layer formed on the electrode was presented based on the experimental results [13]. Our method involves the measurement of nonlinear electrochemical properties in which higher harmonics of FFT are measures of the adsorption characteristics [14–17]. In fact, our previous study showed that the differential capacitance curves are closely related to the species of the protein adsorbed onto a solid surface as well as the packing state of proteinaceous layers [14]. The QCM quantitatively provides the information of the adsorbed amount and is insensitive to the adsorption state. In contrast, electrochemical nonlinearity provides qualitative information on the adsorption state of the protein such as the differential capacitance and conductance. Thus, the present method will provide invaluable information on the adsorption state of the protein.

In this paper, i–v relationships measured during the adsorption of BSA, gelatin and their thiol derivatives on Au electrodes were analyzed by the electrochemical nonlinear method. We summarize our experimental results as follows.

(1) The higher harmonics depended on the concentration of the protein, thiol modification and incubation time.

(2) A much lower degree of hysteresis of the i–v loop was observed for the two thiol-derivatized proteins than for the nonmodified ones (Fig. 3). A small, significant time-dependent change of the i–v loop was observed irrespective of species or thiol modification.

(3) However, higher harmonics of the real part and the imaginary parts in FFT clearly differentiated between the time-dependent electrochemical responses, reflecting the adsorption characteristics of non-modified proteins and their thiol derivatives (Figs. 4–6).

(4) A much lower voltage dependency of capacitance and conductance was observed for the two thiol-derivatized proteins than for the nonmodified ones (Fig. 6). In addition, QCM measurement showed that the adsorption and desorption of nonmodified proteins on the Au surface are reversible, whereas irreversible adsorption on the Au surface occurred for thiol-derivatized proteins. These results strongly indicate that thiol-derivatized proteins are more firmly adsorbed on Au surfaces than nonmodified ones, and that the difference in electrochemical responses may be responsible for the difference in adsorption state, as will be described below.

The adsorption state resulting from physisorption allows a high degree of freedom in movement which includes rotational and lateral movements and des-

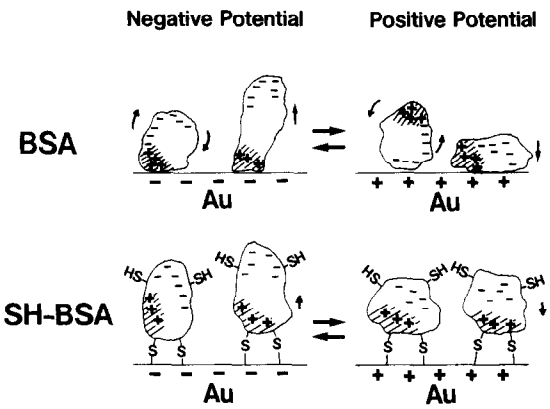

Fig. 9. Schematic representation of the adsorption state of BSA and SH–BSA given at the applied electrical potential.

orption and readsorption. Upon polarity change of voltage, adsorption sites of proteins are changed by molecular rotation to achieve maximal electrostatic interaction with the electrode, since many proteins have ionic domains clustered with negatively charged side-chains of amino acid residues such as glutamic acid or aspartic acid and positively charged ones such as lysine or histidine. When a positive electrical potential is applied to the electrode, a negative ionic domain of an adsorbed protein rotates to achieve maximum interaction with the electrode surface, and when a negative electrical potential is applied, positive ionic domains will relocate on the electrode. This configurational change upon polarity-induced rotation of the adsorbed protein may result in the high degree of hysteresis of the i–v loop when the scan speed of the voltammetric measurement is high, and results in high voltage dependency of capacitance and conductance as schematically illustrated in Fig. 9. In contrast, the adsorption configuration of chemisorbed proteins is fixed on surfaces. Therefore, chemisorbed proteins respond poorly to polarity change of the applied potential, and a slight degree of deformation induced by polarity change of electrical potential may be expected. This results in a low degree of hysteresis of the i–v loop and minimal voltage-dependent conductance and capacitance as experimentally observed (Figs. 4–6). In addition, the packing density of the proteins affects the density of the double layer formed by the hydrophilic domains of the protein and the conductance of the electrode surface depending on the hydrophobicity of the protein, and then both differential capacitance and voltage-dependent conductance are changed depending on the packing density of the protein. The electrochemical nonlinearity discussed in this paper may provide invaluable physicochemical information on the adsorption state of proteins, which may deepen our understanding of protein adsorption and serve as a guide to achieve a logical surface design for better biocompatibility.

Appendix A

Suppose that an electrochemical system consists of a parallel circuit with voltage-dependent capacitor and conductor as simple nonlinear elements given by Eqs. (1) and (2) [14,15]. When a sinusoidal electrical potential ($V(t) = E_0 + E_a \cos \omega_0 t$) is applied to the parallel circuit, the current through the conductor $I_G(t)$ and the current through the capacitor $I_C(t)$ are given by Eqs. (A1) and (A2), respectively:

$$
\begin{aligned}
I_G(t) &= V(t)G(V) \\
&= (E_0 + E_a\cos\omega_0 t)\{G_0 + G_1(E_0 + E_a\cos\omega_0 t) \\
&\quad + G_2(E_0 + E_a\cos\omega_0 t)^2 \\
&\quad + G_3(E_0 + E_a\cos\omega_0 t)^3\} \\
&= G_0E_0 + G_1\{E_0^2 + (1/2)E_a^2\} \\
&\quad + G_2E_0\{E_0^2 + (3/2)E_a^2\} \\
&\quad + G_3\{E_0^4 + 3E_0^2E_a^2 + (3/8)E_a^4\} \\
&\quad + [G_0E_a + 2G_1E_0E_a \\
&\quad + 3G_2E_a\{E_0^2 + (1/4)E_a^2\} \\
&\quad + G_3E_0E_a\{4E_0^2 + 3E_a^2\}]\cos\omega_0 t \\
&\quad + (1/2)[G_1 + 3G_2E_0 \\
&\quad + 6G_3E_a(E_0^2 + E_a)]E_a^2\cos 2\omega_0 t \\
&\quad + E_a^3(G_2 + G_3E_0)\cos 3\omega_0 t \\
&\quad + (1/8)G_3E_a^4\cos 4\omega_0 t \qquad \text{(A1)}
\end{aligned}
$$

$$
\begin{aligned}
I_C(t) &= dQ/dt = (dQ/dV)(dV/dt) \\
&= C(V)(dV/dt) \\
&= \left(C_0 + C_1 V + C_2 V^2 + C_3 V^3\right) \\
&\quad \times d(E_0 + E_a \cos\omega_0 t)/dt \\
&= \left\{C_0 + C_1(E_0 + E_a\cos\omega_0 t)\right. \\
&\quad + C_2(E_0 + E_a\cos\omega_0 t)^2 \\
&\quad \left. + C_3(E_0 + E_a\cos\omega_0 t)^3\right\}(-\omega_0 E_a \sin\omega_0 t) \\
&= -\omega_0 E_a\left[\left\{C_0 + C_1 E_0 + C_2 E_0^2 + C_3 E_0^3\right.\right. \\
&\quad \left. + (1/4) E_a^2 (C_2 + 3C_3 E_0)\right\}\sin\omega_0 t \\
&\quad + (1/2)\left\{\left(C_1 E_a + 2C_2 E_0 E_a + 3C_3 E_0^3 E_a\right)\right. \\
&\quad \left. + (1/2) C_3 E_a^3\right\}\sin 2\omega_0 t \\
&\quad + (1/4) E_a^2 (C_2 + 3C_3 E_0)\sin 3\omega_0 t \\
&\quad \left. + (1/8) E_a^3 C_3 \sin 4\omega_0 t\right] \qquad \text{(A2)}
\end{aligned}
$$

The total current $I(t)$ through the voltage source becomes

$$I(t) = I_G(t) + I_C(t) \qquad \text{(A3)}$$

Substituting Eqs. (A1) and (A2), and experimental conditions $E_0 = 0$ V, $E_a = 0.3$ V, $\omega_0 = 2\pi f$ and $f = 0.5$ Hz into Eq. (A3), we obtain Eq. (3).

References

[1] J.D. Andrade, in J.D. Andrade (Ed.), Protein adsorption, Surface and Interfacial Aspects of Biomedical Polymers, Vol. 2, Plenum Press, New York, 1985, Chapter 1.

[2] J.D. Andrade and V. Hlady, Adv. Polym. Sci., 79 (1986) 1.

[3] G.A. Bornzin and I.F. Miller, J. Colloid Interface Sci., 86 (1982) 539.

[4] K.K. Chittur, D.J. Fink, R.I. Leininger and T.B. Hutson, J. Colloid Interface Sci., 111 (1986) 419.

[5] P. Bernabeu, A. de Cesare and A. Caprani, J. Electroanal. Chem., 265 (1989) 261.

[6] A.V. Elgersma, R.L.J. Zsom, W. Norde and J. Lyklema, J. Colloid Interface Sci., 138 (1990) 145.

[7] E.W. Wollman, C.D. Frisbie and M.S. Wrighton, Langmuir, 9 (1993) 1517.

[8] L. Sun, B. Johnson, T. Wade and R.M. Crooks, J. Phys. Chem., 94 (1990) 8869.

[9] R.G. Nuzzo, B.R. Zegarski and L.H. Dubois, J. Am. Chem. Soc., 109 (1987) 733.

[10] R.G. Nuzzo, F.A. Fusco and D.L. Allara, J. Am. Chem. Soc., 109 (1987) 2358.

[11] C.D. Bain, E.B. Troughton, Y.-T. Tao, J. Evall, G.M. Whitesides and R.G. Nuzzo, J. Am. Chem. Soc., 111 (1989) 321.

[12] B. Venkataraman, G.W. Flynn, J.L. Wilbur, J.P. Folkers and G.M. Whitesides, J. Phys. Chem., 99 (1995) 8684.

[13] F. Lacour, R. Torresi, C. Gabrielli and A. Caprani, Coll. Sur. B: Biointer., 1 (1993) 251.

[14] S. Nakata, K. Yoshikawa and T. Matsuda, Biophys. Chem., 42 (1992) 213.

[15] S. Nakata, K. Yoshikawa, M. Shoji, H. Kawakami and T. Ishii, Biophys. Chem., 34 (1989) 201.

[16] S. Nakata, Y. Kaneda and K. Yoshikawa, Sens. Mater., 4 (1992) 101.

[17] N. Mohri, Y. Katsuya, S. Nakata and K. Yoshikawa, Bull. Chem. Soc. Jpn., 66 (1993) 1328.

[18] M. Hara, Y. Iwakabe, K. Tochigi, H. Sasabe, A.F. Garito and A. Yamada, Nature, 344 (1990) 228.

[19] M. Thompson, C.L. Arthur and G.K. Dhaliwal, Anal. Chem., 58 (1986) 1206.

[20] M. Muratsugu, F. Ohta, Y. Miya, T. Hosokawa, S. Kurosawa, N. Kamo and H. Ikeda, Anal. Chem., 65 (1993) 2933.

[21] S. Imai, H. Mizuno, M. Suzuki, T. Takeuchi, E. Tamiya, F. Mashige, A. Ohkubo and I. Karube, Anal. Chim. Acta, 292 (1994) 65.

[22] A.F. Habeeb, Anal. Biochem., 14 (1966) 328.

[23] W. Carius, J. Colloid Interface Sci., 57 (1976) 301.

[24] F. van der Touw and M. Mandel, Biophys. Chem., 2 (1974) 231.

[25] L.L. Hause, R.A. Momorowski and F. Cayon, IEEE Trans. Biomed. Eng., 28 (1981) 403.

[26] A.J. Bard and L.R. Faulkner, Electrochemical Methods, Wiley, New York, 1980.

[27] S.N. Magonov and H.-J. Cantow, J. Appl. Polym. Sci., Appl. Polym. Symp., 51 (1992) 3.